Application Note

Cell Analysis

Agilent

Trusted Answers

Autofluorescence Subtraction with the Agilent NovoCyte Opteon Spectral Flow Cytometer

Author

Xiaohuan Wang, Ming Lei, Yan Lu, Peifang Ye, Garret Guenther, Nancy Li, Agilent Technologies, Inc.

Abstract

Cells exhibit autofluorescence due to intrinsic fluorescent biological molecules, which can interfere with signal resolution during fluorescence marker detection. To improve fluorochrome resolution, spectral flow cytometers, unlike conventional flow cytometers, capture the full fluorochrome emission spectrum. Autofluorescence can be treated like a background signal and extracted from fluorochrome-labeled cell signals. In this study, unmixed results with and without autofluorescence extraction are compared across different samples, showing that proper autofluorescence characterization and extraction improve signal resolution and enhance unmixing accuracy. Complex autofluorescence identification strategies are needed for samples including heterogeneous autofluorescence signals, while simpler strategies are sufficient for samples with homogeneous autofluorescence signals. The Agilent NovoCyte Opteon spectral flow cytometer, combined with the Agilent NovoExpress software, facilitates effective autofluorescence subtraction for improved data quality and analysis.

Introduction

Cells exhibit autofluorescence due to the presence of various endogenous molecules, such as aromatic amino acids, lipofuscins, pyridine nucleotides, and flavin coenzymes, which emit fluorescence when excited by specific wavelengths of ultraviolet or visible light.[1] The levels of cellular autofluorescence can vary depending on the cell type, metabolic state, and even experimental conditions.[2] Traditionally, cellular autofluorescence has been seen as a significant challenge in flow cytometry, as it generates extraneous noise and lowers the sensitivity of fluorophore detection. Cell populations with high autofluorescence may be mistaken as positive for a given fluorochrome or antigen.[3] In spectral flow cytometry, autofluorescence and fluorochrome signals can be separated, improving the fidelity of marker quantification.[4] Spectral flow cytometry uses an array of detectors that span a wide range of emission wavelengths, capturing the spectral characteristics of fluorochromes and autofluorescence.[5] By identifying the autofluorescence characteristics of each sample, it is possible to distinguish between autofluorescence and fluorochrome signals, ensuring that two are not conflated.[2, 5] Additionally, in samples with high autofluorescence, fluorochrome signals with emission peaks close to the autofluorescence signal can be distinguished, improving fluorescence detection resolution.[2] The Agilent NovoCyte Opteon spectral flow cytometer offers up to five lasers and 73 detectors, enabling high-resolution data acquisition and autofluorescence spectrum characterization. The NovoExpress software facilitates the identification of distinct autofluorescence spectra in unstained samples. Tools such as reference spectrum similarity aid in identifying similar autofluorescence spectra, helping users avoid redundant autofluorescence spectra in the unmixing, which can lead to unnecessary spreading error.

This application note elucidates the diverse autofluorescence characteristics across different samples and demonstrates how the removal of autofluorescence significantly enhances result resolution and accuracy. Strategies to identify distinct autofluorescence characteristics using NovoExpress software are also outlined. The samples tested included fresh and stabilized human blood, as well as mouse splenocytes and lung cells—samples with homogenous or heterogeneous autofluorescence properties. Results show complex autofluorescence extraction strategies are needed for samples with heterogeneous autofluorescence signals, while simpler strategies are sufficient for those with homogeneous signals. The NovoCyte Opteon spectral flow cytometer, combined with the NovoExpress software, facilitates effective autofluorescence extraction for optimal analysis.

Experimental

Instrument configuration

NovoCyte Opteon UVBYR spectral flow cytometer featuring five lasers (349, 405, 488, 561, and 637 nm), forward scatter (FSC), blue laser excited side scatter (BSSC), violet laser excited side scatter (VSSC), and 70 fluorescence detectors

Human blood sample preparation

Freshly collected human peripheral blood anticoagulated with ethylenediaminetetraacetic acid (EDTA) or stabilized human peripheral blood (CD-Chex Plus) were incubated with the appropriate quantity of antibodies for 15 minutes (Table 1 or Table 2). Red blood cells were lysed with 1x AceaLyse solution (Table 3). The samples were centrifuged at 300 *x g* for five minutes. The supernatant was removed and cells washed with phosphate buffered saline (PBS) once. The pellets were resuspended with 1% paraformaldehyde (PFA) in PBS.

Table 1. Antibodies in the fresh human blood immunophenotyping panel.

Specificity	Fluorochrome	Clone	Vendor	Part Number
CD45	Brilliant Violet 510	HI30	Biolegend	304036
CD4	Brilliant Violet 421	RPA-T4	Biolegend	300532
CD3	PerCP-Cy5.5	SK7	Agilent	8931015
CD8	APC	SK1	Agilent	8931025
CD19	PE-Cy7	HIB19	Agilent	8930015
CD16	PE	3G8	Agilent	8930005
CD56	PE	HCD56	Biolegend	318306

Table 2. Antibodies in the fresh human blood immunophenotyping panel.

Specificity	Fluorochrome	Clone	Vendor	Part Number
CD45	Brilliant Violet 510	HI30	Biolegend	304036
CD4	Brilliant Violet 421	RPA-T4	Biolegend	300532
CD8	Pacific Blue	SK1	Biolegend	344718
CD3	PerCP-Cy5.5	SK7	Agilent	8931015
CD20	FITC	2H7	Agilent	8730070
CD16	PE	3G8	Agilent	8930005
CD56	PE	HCD56	Biolegend	318306

Table 3. Other reagents used.

Reagent	Vendor	Part Number
AceaLyse solution	Agilent	894B604
Phosphate buffered saline (PBS)	GENOM BIO	GNM20012-2
Paraformaldehyde (PFA), 4% in PBS	Aladdin	P395744-100mL
CD-Chex Plus	Streck	213323

Mouse spleen and lung sample preparation

Mouse spleen and lung tissue were cut into small pieces. Mouse spleen tissue was gently pressed, and lung tissue was digested with enzymes. Homogenized samples were passed through 70 µm nylon meshes, and red blood cells (RBC) were lysed using 1x RBC lysis buffer (Table 6). Following that, cells were collected and stained with antibody mixtures in Table 4 or 5 at 4° C for 30 minutes. Samples were centrifuged at 300 *x g* for five minutes. Supernatants were discarded, and cells were washed once with PBS containing 2% fetal bovine serum (FBS). Pellets were resuspended with 1% PFA in PBS. Dead cells were identified with propidium iodide (PI) or Live/Dead Blue reagent.

Table 4. Antibodies in the spleen cell immunophenotyping panel.

Specificity	Fluorochrome	Clone	Vendor	Part Number
Live/Dead	PI	NA	Thermo fisher	V13241
CD4	PE-Fire640	GK1.5	Biolegend	100481
CD11b	PE-Cy7	M1/70	Biolegend	101215
NK1.1 (C57)	APC	PK136	Biolegend	108709
CD19	Alexa Fluor 700	6D5	Biolegend	115527
CD3	BV421	17A2	Biolegend	100228
CD8a	BV570	53-6.7	Biolegend	100740
CD45.2	FITC	104	Biolegend	109805

Table 5. Antibodies in the lung cell immunophenotyping panel.

Specificity	Fluorochrome	Clone	Vendor	Part Number
Live/Dead	Live Dead Blue	NA	Thermo fisher	423105
CD45	PerCP	30-F11	Biolegend	103129
Sca-1	APC-Fire750	D7	Biolegend	108146
EpCAM (CD326)	eFluor450	G8.8	Thermo fisher	48-5791-82
CD11b	PE-Cy7	M1/70	Biolegend	101215
Ly6G	BV605	1A8	Biolegend	127639
Siglec-F	PE-CF594	E50-2440	BD	562757
F4/80	Kiravia Blue520	BM8	Biolegend	123162
CD11c	BUV805	N418	BD	749038
CD103	PE	2E7	Biolegend	121405
MHC II	BV785	M5/114.15.2	Biolegend	107645
CD64	APC	X54-5/7.1	Biolegend	139306
CD24	BV510	M1/69	Biolegend	101831
Ly6C	BV711	HK1.4	Biolegend	128037

Table 6. Other reagents used.

Reagent	Vendor	Part Number
Hanks' balanced salt solution (HBSS)	Gibco	14025-092
Phosphate buffered saline (PBS)	GENOM BIO	GNM20012-2
Paraformaldehyde (PFA), 4% in PBS	Aladdin	P395744
Fetal bovine serum (FBS)	Gibco	10091-148
EDTA, 0.5 M pH 8.0	Invitrogen	AM9260G
TruStain FcX PLUS	Biolegend	156603
Brilliant Stain Buffer Plus	BD Biosciences	66385
Collagenase D	Roche	11088858001
DNase I	Sigma-Aldrich	D4513-1VL
1x RBC lysis buffer	Invitrogen	00-4333-57

Identify and set the autofluorescence spectra

The NovoExpress software uses fluorescence signal patterns from unstained samples to enable the identification of distinct autofluorescent populations. These populations can be conveniently designated as autofluorescence controls via the right-click menu or through the Reference Control Specimen Setup window. Users can configure autofluorescence controls for a single sample type or for multiple, including cells, beads, or tissue-derived samples. In the fluorochrome settings panel, corresponding unstained samples can be easily selected for each stained sample. For detailed instructions, please refer to the NovoExpress software guide.

Results

The autofluorescence spectra of different samples

Levels of cellular autofluorescence can vary depending on several factors, such as cell type, size, metabolic state, and experimental conditions. Figure 1 shows the fluorescence intensity distribution of various unstained samples over all fluorescence detection channels. Notably, while individual cell populations from unstained stabilized human peripheral blood have distinct autofluorescence intensities, their signatures are similar (Figure 1A). In contrast, the autofluorescence signatures of different populations of unstained mouse lung cells vary dramatically (Figure 1B). When the sample types are the same, the autofluorescence of stabilized human peripheral blood lymphocytes is much stronger than that of fresh human peripheral blood lymphocytes (Figures 1C and D).

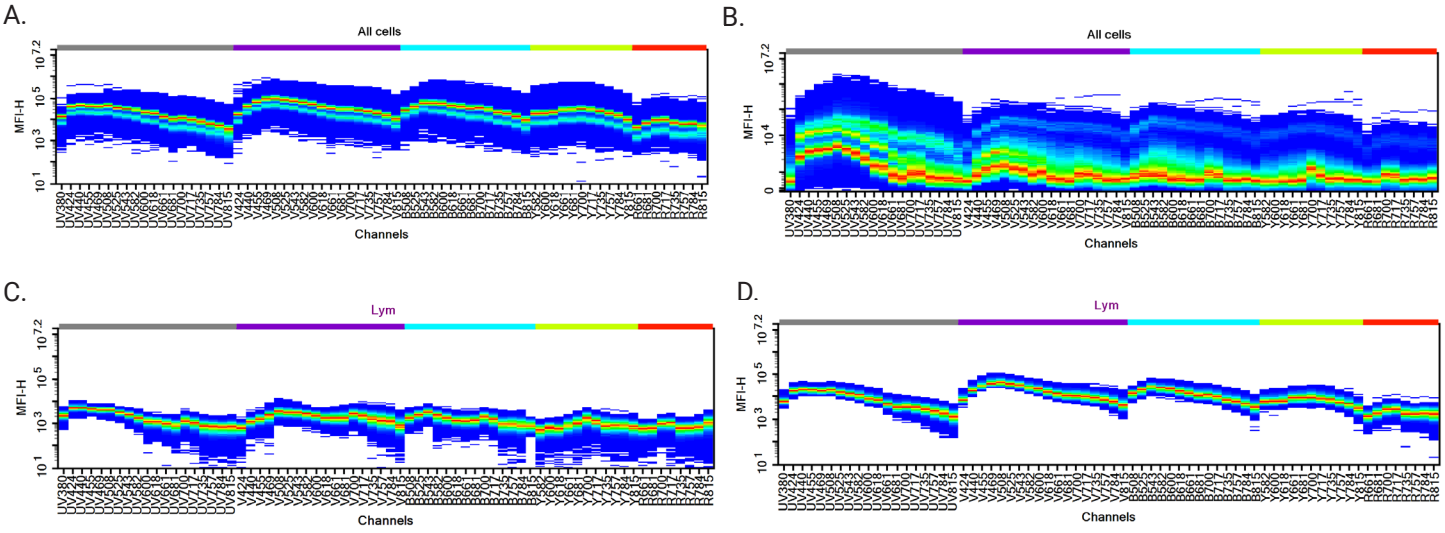

Figure 1. Density spectrum plots of unstained populations from different samples. (A) Unstained stabilized human blood cells with all populations included. (B) Unstained mouse lung cells with all populations included. (C) Lymphocytes from an unstained fresh human blood sample. (D) Lymphocytes from an unstained stabilized human blood sample.

Autofluorescence subtraction from fresh/stabilized human blood cells

Given the high similarity of the autofluorescence signatures of different populations in human blood samples, including one autofluorescence spectrum in the unmixing process for autofluorescence extraction is enough. For stabilized human blood cells or fresh human blood cells, lymphocytes were gated based on the FSC/BSSC plot and set as an autofluorescent population (Figures 2A and B, fresh blood sample as an example). Since the autofluorescence signal intensity is low for a fresh blood sample, (Figure 1C), there was no discernible difference between the unmixed results with and without autofluorescence subtraction included in the unmixing process (Figure 2C). Consequently, for samples exhibiting homogeneous and low autofluorescence signals, including autofluorescence spectra in the unmixing process is optional.

In stabilized human blood samples, however, the autofluorescence signals are significantly stronger. In full-stained samples, incorporating autofluorescence subtraction into the unmixing process can effectively eliminate autofluorescence background, enhancing cell population distinction (Figure 2D). Consequently, when the population of interest exhibits strong homogeneous autofluorescence, including autofluorescence subtraction in the unmixing step can greatly enhance separation and accuracy when identifying specific cell populations.

Note that things such as disease states, activation conditions and drug treatments, may affect blood sample autofluorescence, requiring additional investigation of the autofluorescence intensity and characteristics.

Autofluorescence subtraction from mouse spleen cells

In Figure 3A, the spectral density plot of unstained mouse splenocytes reveals that most cells exhibit consistent autofluorescence signatures, while minor subpopulations display divergent autofluorescence profiles. To systematically characterize all autofluorescence-distinct cell populations, we first gated the cell population of interest using an FSC/SSC plot to exclude debris and nonviable cells. Subsequent analysis of spectral density plots and bivariate plots of channels with differential autofluorescence signals (not shown) identified two populations with distinct autofluorescence signatures: A1 and B (Figure 3B). To validate their spectral uniqueness, we employed a spectral similarity matrix in NovoExpress software, which quantifies divergence (similarity ≤ 0.95 denotes distinct populations). Notably, A1 and B exhibited a low similarity score of 0.42, confirming significant spectral dissimilarity (Figures 3C and 3D). These validated populations (AF-A1 and AF-B) were subsequently incorporated into the spectral unmixing workflow.

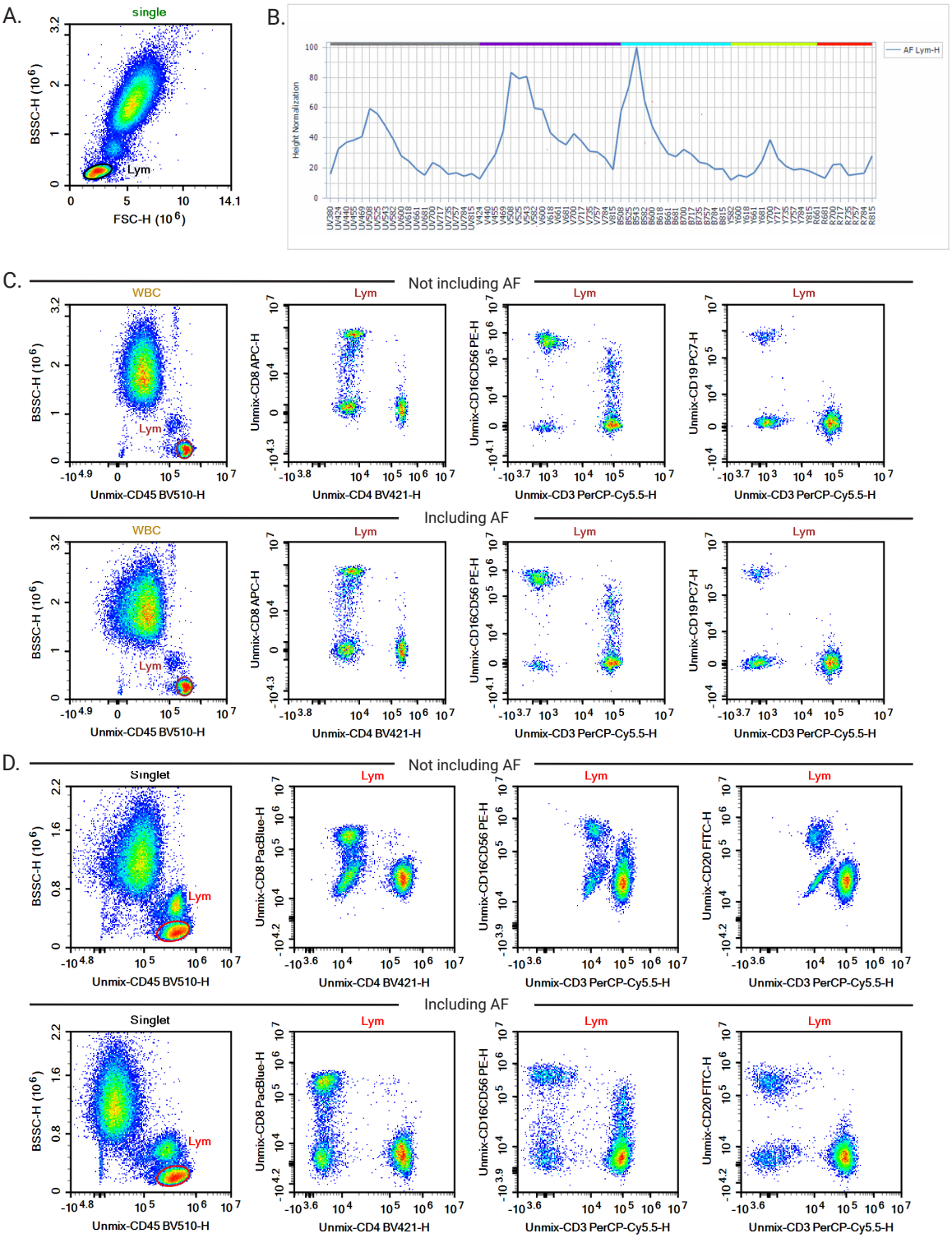

Figure 2. Effects of autofluorescence extraction for seven-color human blood immunophenotyping panels. (A) The gate of lymphocytes of an unstained fresh human blood sample in the FSC/BSSC density plot. (B) Spectrum signature of lymphocytes in A. Comparison of unmixing results for full-stained samples with or without autofluorescence spectra included, (C) fresh human blood, and (D) stabilized human blood.

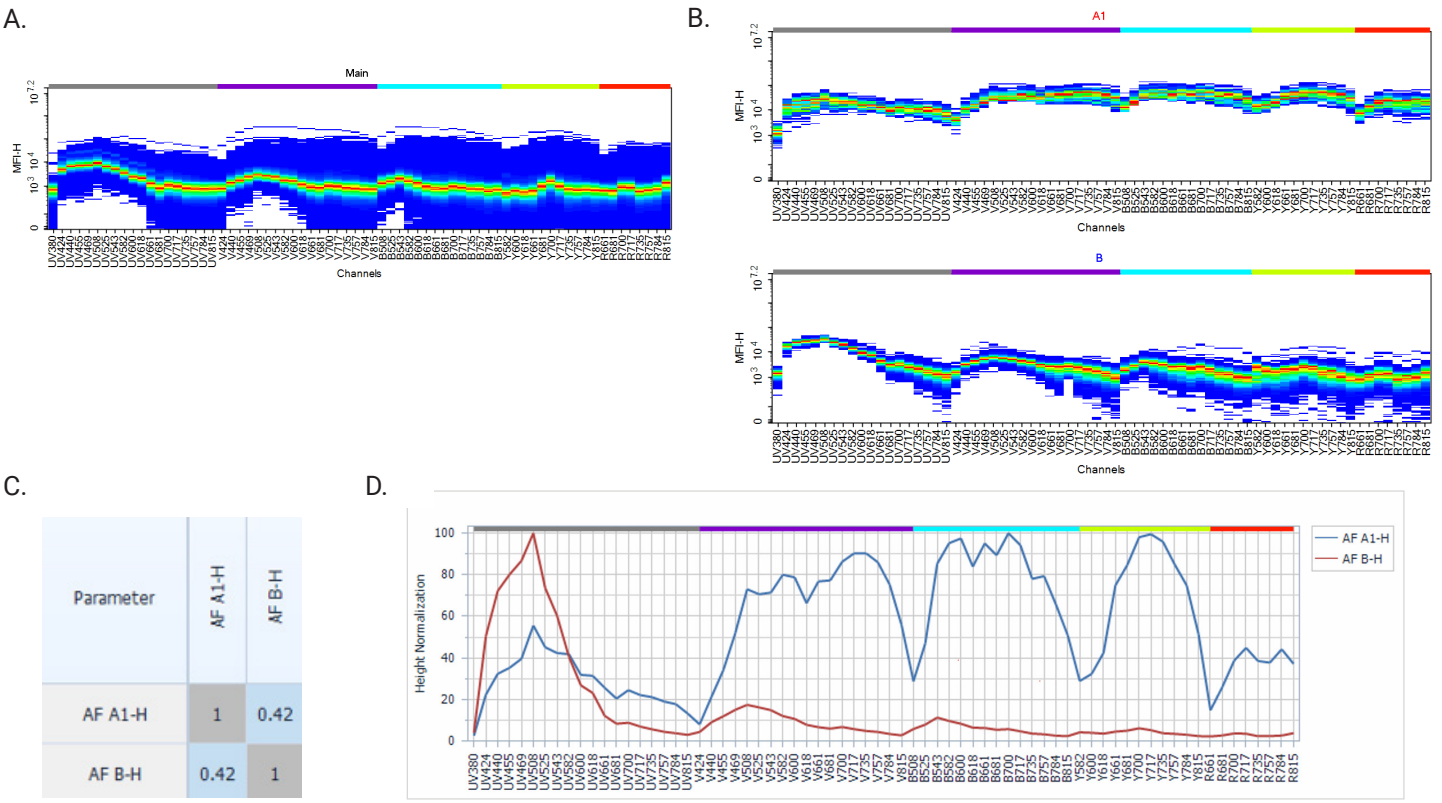

Figure 3. Identifying distinct autofluorescence signatures in an unstained mouse splenocyte sample. (A) Spectral density plot of the main population. (B) Spectral density plot of the A1 and B populations. (C) AF A1 and AF B spectral similarity matrix. (D) Spectra of AF A1 and AF B.

After characterizing the autofluorescent populations, we compared the unmixing results with and without the inclusion of these autofluorescence spectra. In the unstained (Figure 4A), CD8a BV570 single-stained (Figure 4B), and full-stained samples (Figure 4C), not including autofluorescence spectra from unmixing created messy false-positive populations (indicated by red arrow). Including AF-A1 and AF-B spectra in the unmixing process eliminated these artifacts, resulting in accurate immunophenotyping. Finally, the biological analysis of the full-stained sample was shown in Figure 5, where the immune subpopulations were accurately identified.

Autofluorescence subtraction from mouse lung cells

There were highly heterogeneous and strong autofluorescence signals in the unstained mouse lung sample, and it was not possible to distinguish individual populations from the FSC/BSSC plot. To identify all populations with different autofluorescence signatures, all cells of interest were gated as **Main** from FSC/SSC, and the spectral density plot of the **Main** population revealed peak autofluorescence signals in UV/V channels (Figure 6A). Channels exhibiting strong or heterogeneous autofluorescence signals were used to distinguish autofluorescent populations. Four populations (A to D) were identified via UV784/UV424 density plot, with hierarchical gating in other channels ensuring uniform autofluorescence per gate (Figure 6B). Populations were filtered using spectral similarity (≤ 0.95), retaining only the highest-intensity populations from similar clusters (Figure 6C). Final unmixing included four unique autofluorescence spectra (A2, B1, B3, C1; Figure 6D).

After identifying the four autofluorescence spectra, it was verified that the unmixing results of the single-stained samples were accurate. Then, the spectral matrix was applied to the full-stained sample. The comparison between unmixing with and without autofluorescence involved is illustrated in Figure 7. In the unstained (Figure 7A), CD24 BV421 single-stained (Figure 7B), and full-stained samples (Figure 7C), not including autofluorescence from unmixing created messy false-positive populations (indicated by cyan). Including the four autofluorescence spectra in the unmixing process eliminated these artifacts, enhancing the immunophenotyping accuracy. Finally, the biological analysis of the full-stained sample is shown in Figure 8, where the immune subpopulations were accurately distinguished.

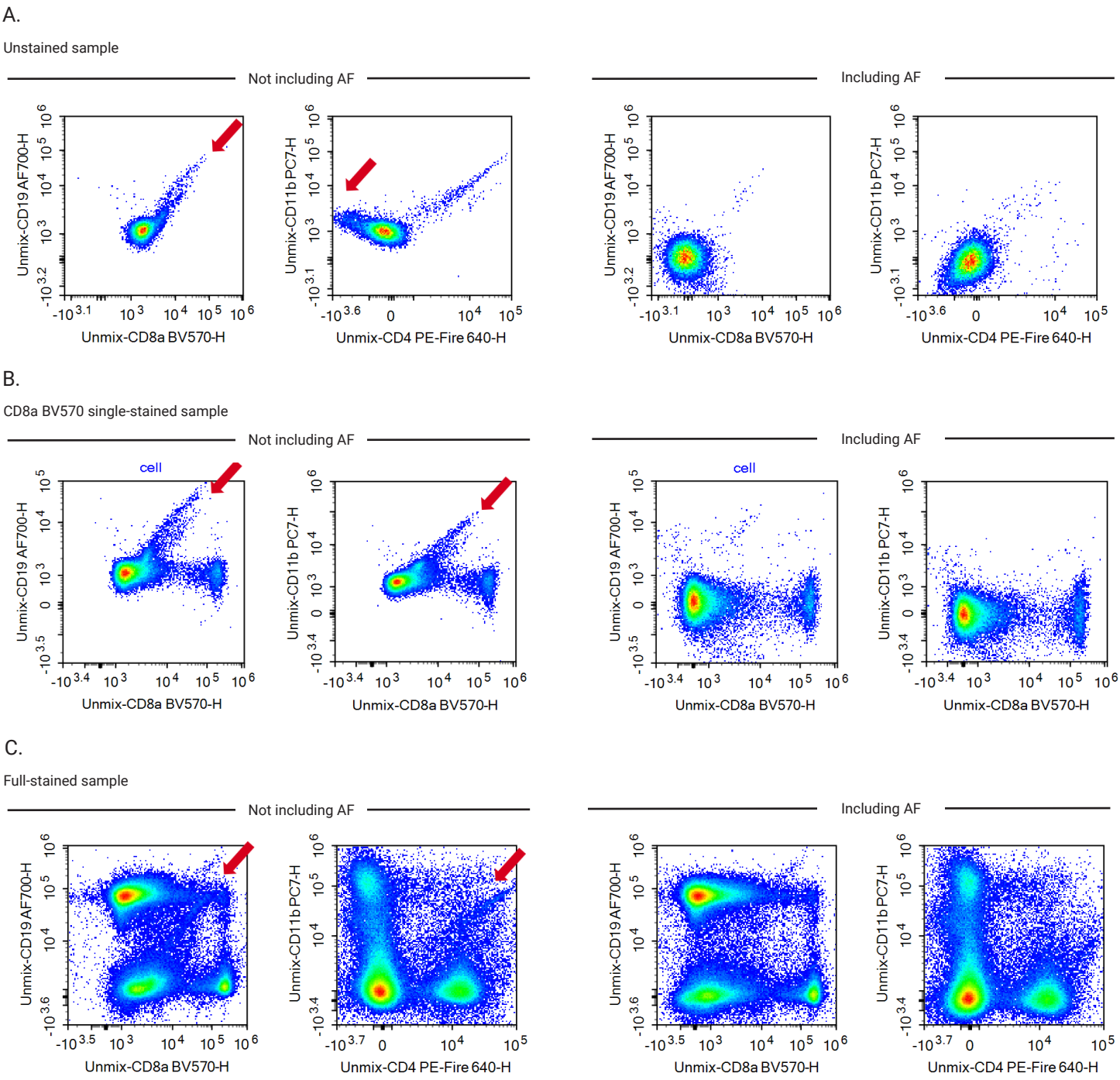

Figure 4. Effects of autofluorescence extraction for an eight-color mouse spleen cell immunophenotyping panel. Typical plots of an unstained sample (A), a CD8 BV570 single-stained sample (B), and a full-stained sample (C) with or without autofluorescence spectra included in the unmixing workflow were compared.

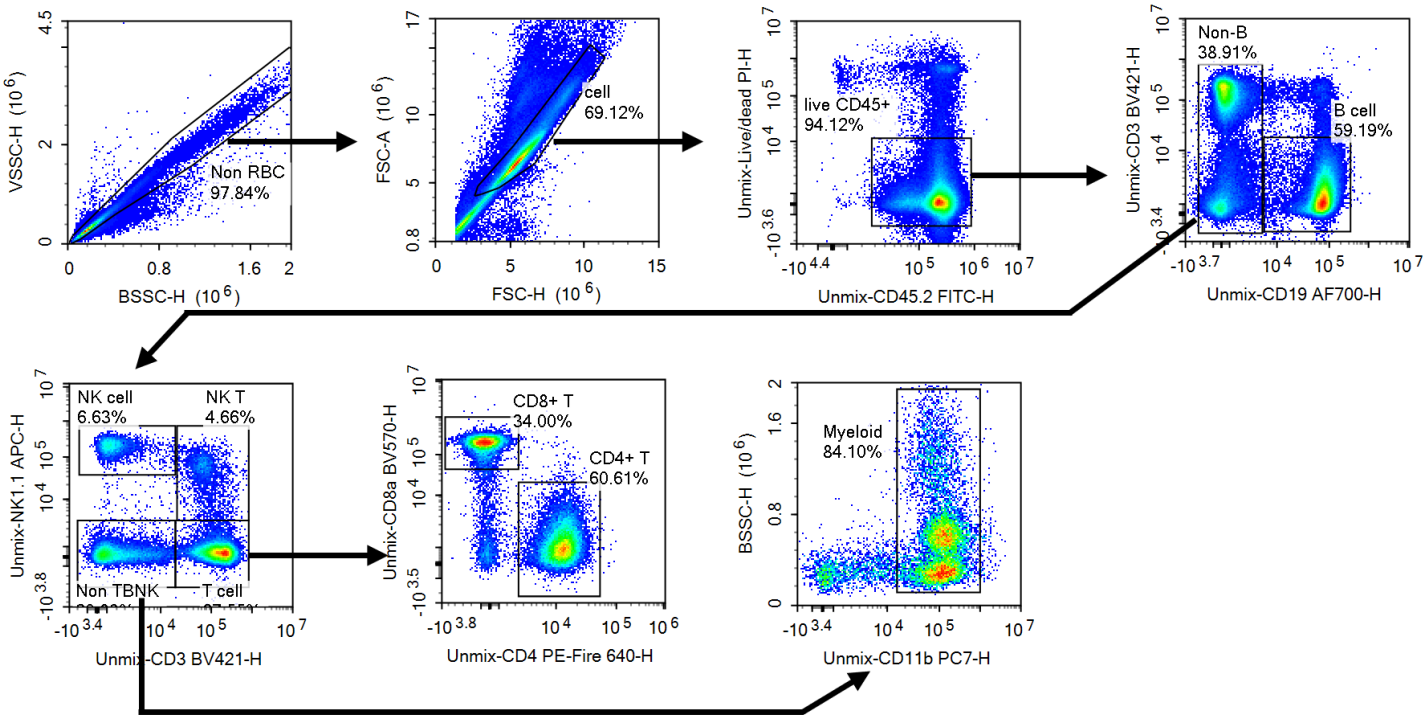

Figure 5. An example of mouse spleen cells phenotyping with autofluorescence well eliminated. Sequential gating was applied to identify the following cell populations: B cells, NKT cells, NK cells, CD8a+ T cells, CD4+ T cells, and myeloid cells.

How different autofluorescence properties of negative and positive populations in a single-stained sample interfere with the spectrum calculations

In highly heterogeneous samples with strong autofluorescence, accurately calculating spectra for all fluorochromes from single-stained samples can be challenging. As shown in Figure 9A, the unmixing of the CD24 BV510 single-stained sample was not accurate after subtracting the negative population signal from that of the positive population. Using the spectral density plot of the Main population of the CD24 BV510 single-stained sample (Figure 9B) to calculate the BV510 spectrum indicated there are cell populations with different signal intensities from channel UV424 to UV661, but they do not correspond to the negative or positive population. It is a consequence of the autofluorescence heterogeneity in this population. The reference spectrum calculated by subtracting the negative from the positive signal actually contains the difference in the autofluorescence signal of the negative and positive populations. In this case, it is necessary to identify negative and positive populations with uniform autofluorescence intensity. Selecting channels with strong, distinct autofluorescence signals, and no specific fluorochrome signal can help identify populations with identical autofluorescence.

As shown in Figure 9C, we use a UV757/UV424 density plot to identify the E12 population with uniform autofluorescence intensity. Thus, gating the negative and positive populations under E12 ensures uniform autofluorescence intensity, improving spectrum calculation accuracy for BV510. The unmixing result using the corrected spectrum is shown in Figure 9D.

In some more complex cases, some single-stained samples exhibit only a positive population without a corresponding negative population. In such instances, a more sophisticated approach is required. Negative populations that have uniform autofluorescence intensity with the positive populations must be identified in an unstained sample . For such complex cases, it is recommended to use compensation beads for the single-stained samples.

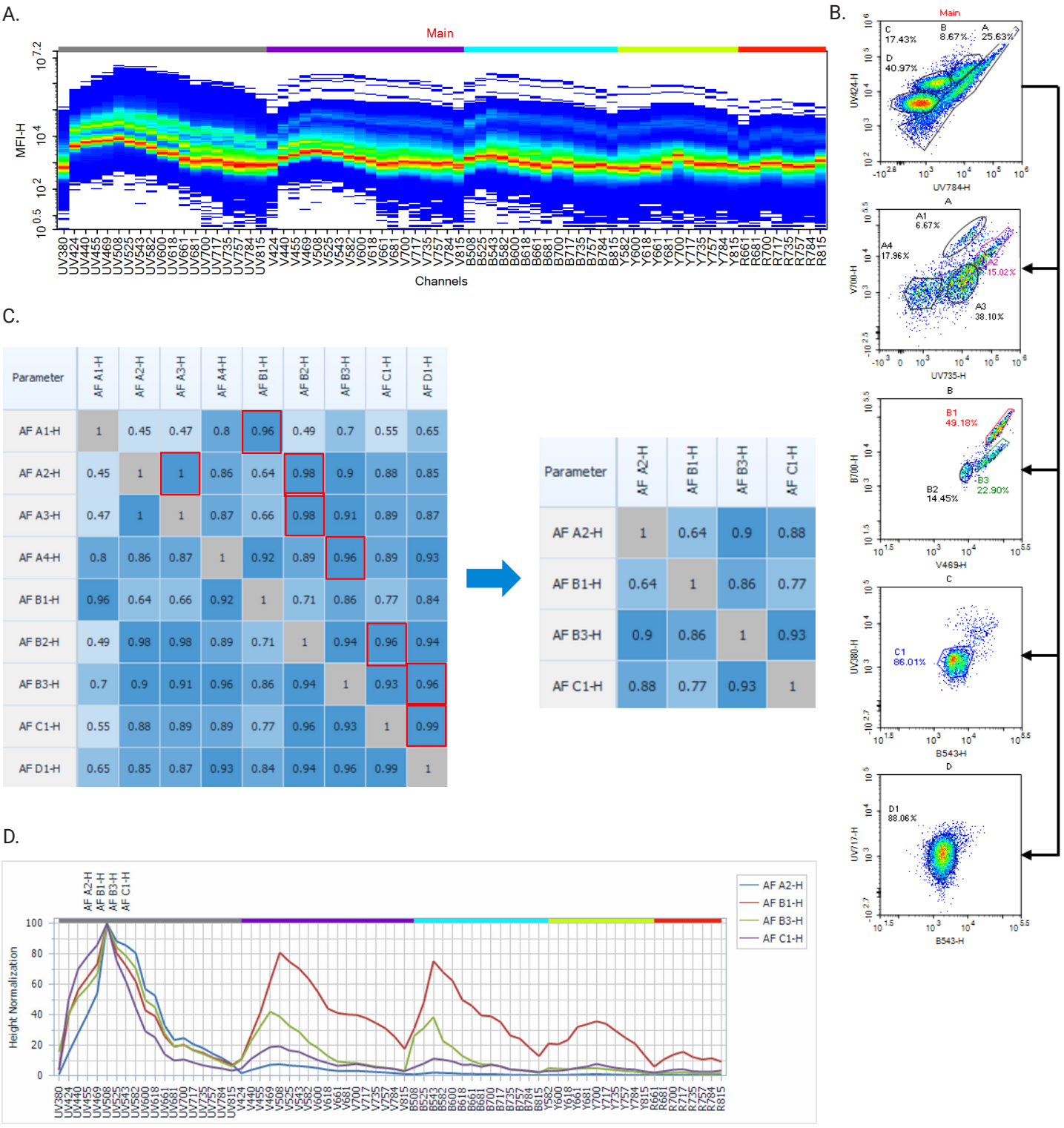

Figure 6. Identifying distinct autofluorescence signatures from an unstained mouse lung sample. (A) The spectral density plot for the **Main** population. (B) Hierarchical gating in various channels was used to identify populations with uniform autofluorescence signatures. (C) Filter autofluorescence spectra via similarity matrix, decreasing from nine spectra (left) to four spectra (right). (D) Spectrum signatures of AF A2, AF B1, AF B3, and AF C1.

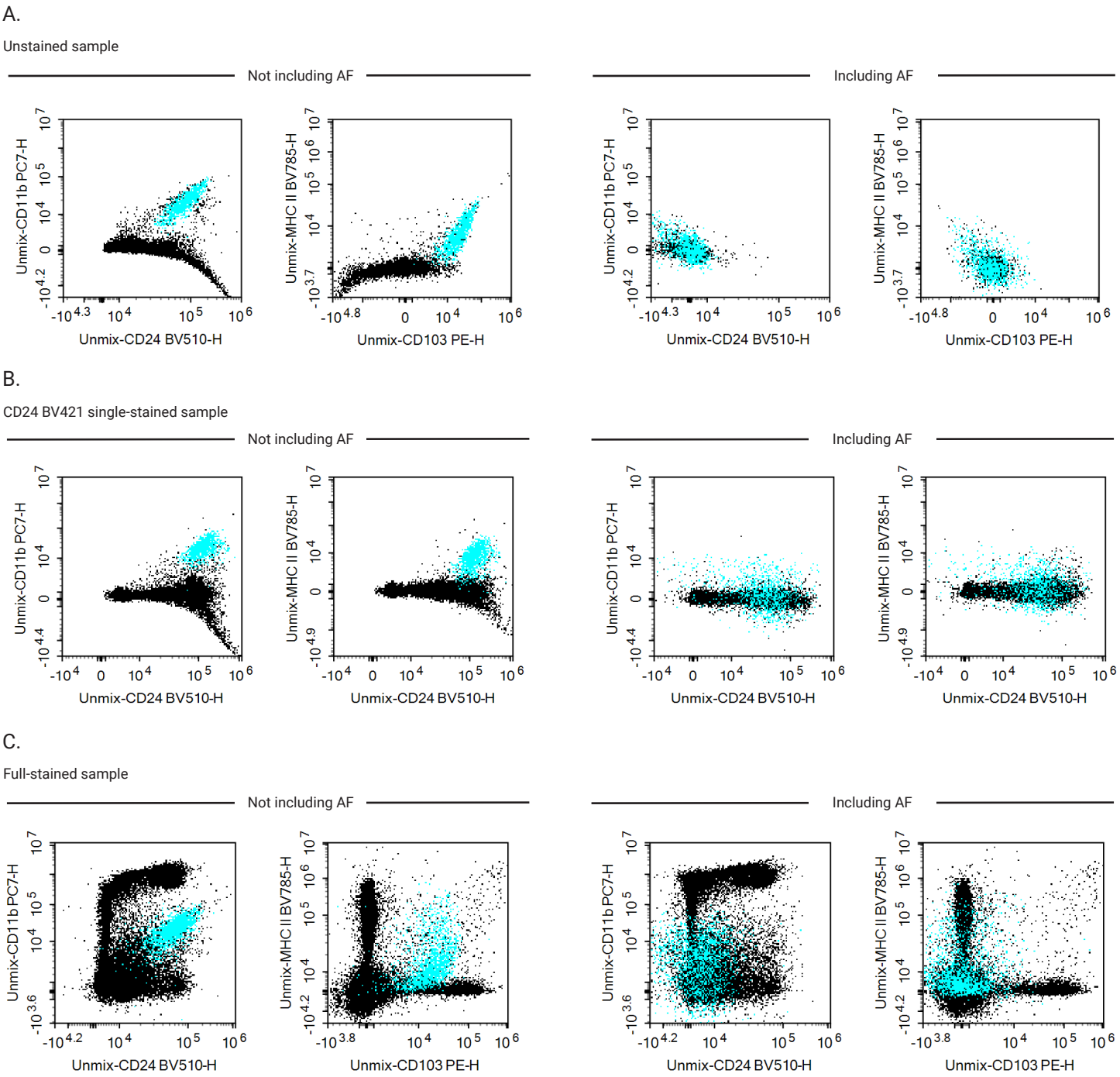

Figure 7. Effects of autofluorescence extraction for a 14-color mouse lung cells immunophenotyping panel. Typical plots of an unstained sample (A), a CD24 BV510 single-stained sample (B), and a full-stained sample (C) with or without autofluorescence spectra included

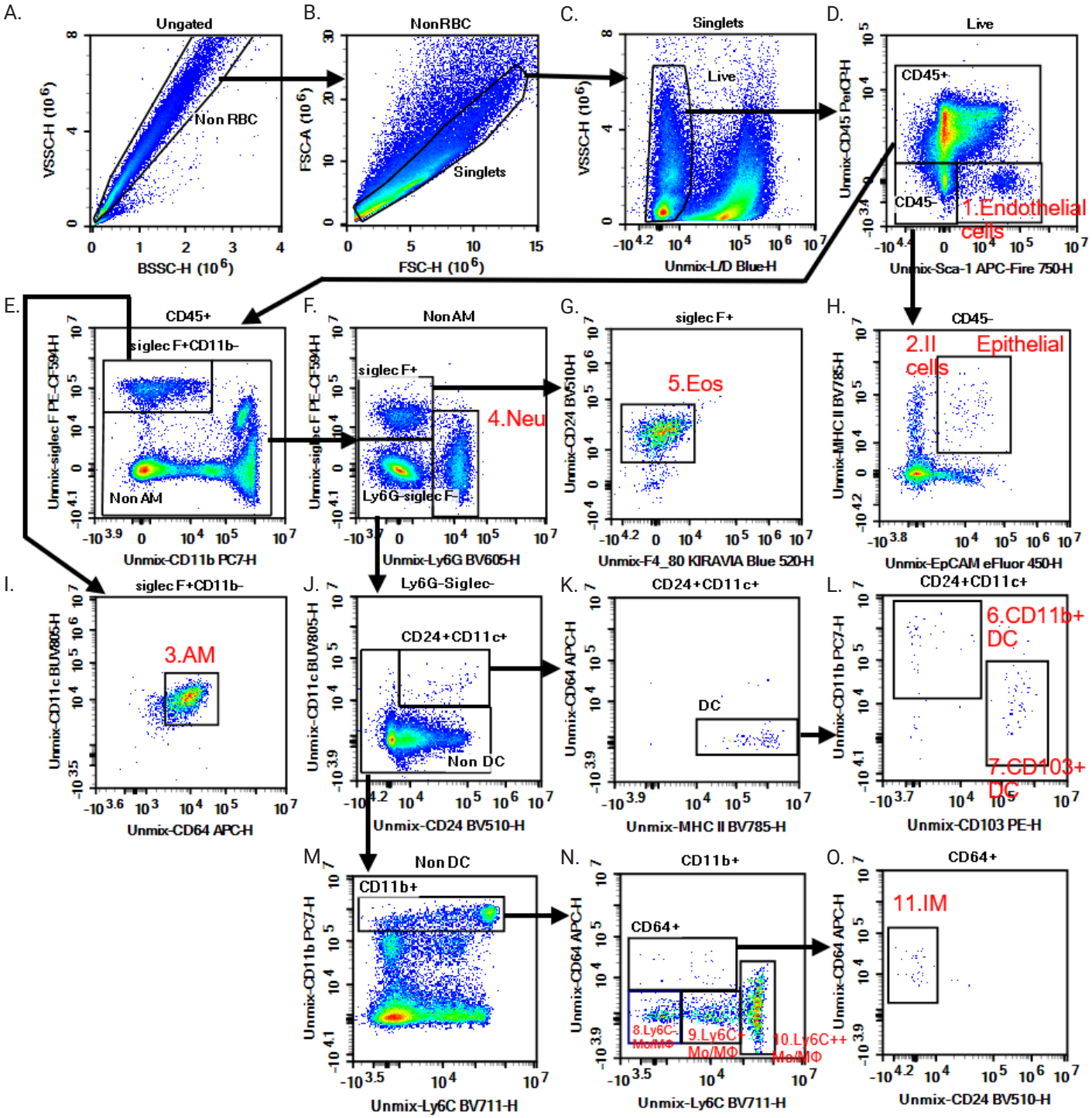

Figure 8. An example of mouse lung cell phenotyping with autofluorescence well eliminated. Hierarchical gating was applied to identify the following cell populations: (1) endothelial cells, (2) type II epithelial cells, (3) alveolar macrophages, (4) neutrophils, (5) eosinophils, (6) CD11b^{+} dendritic cells, (7) CD103^{+} dendritic cells, (8) Ly6C- monocyte/macrophages, (9) Ly6C^{+} monocyte/macrophages, (10) Ly6C^{++} monocyte/macrophages, and (11) interstitial macrophages.

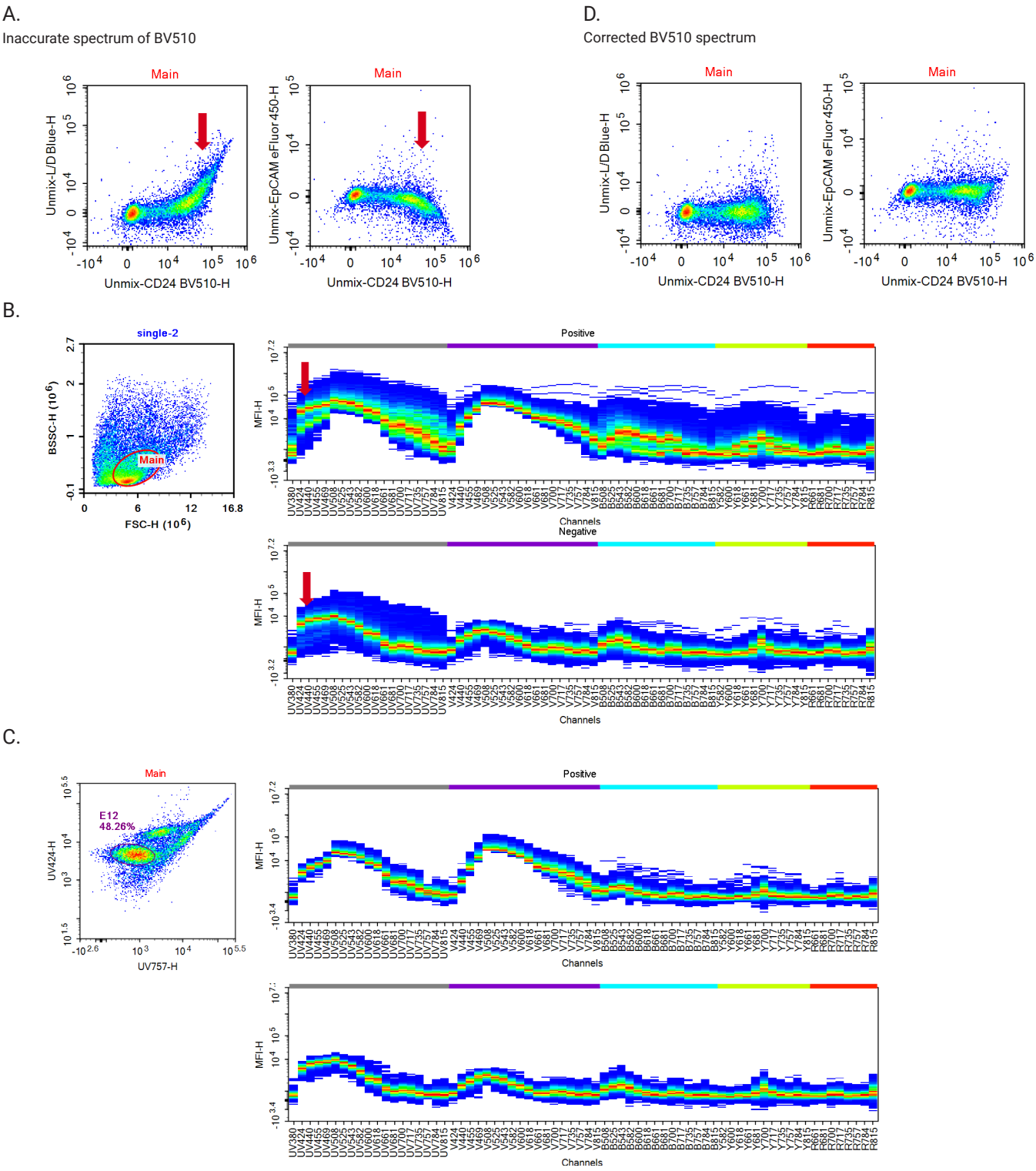

Figure 9. Identifying negative and positive populations with uniform autofluorescence intensities from the CD24 BV510 single-stained mouse lung sample. (A) Unmixed CD24 BV510 single-stained sample data with a simply calculated, not-so-accurate spectrum. (B) The spectral density plot of positive and negative populations within the **Main** population of the CD24 BV510 single-stained sample. (C) Identifying positive and negative populations with identical autofluorescence signals. Gate **E12** from the **Main** population through the UV757/UV424 density plot and check the spectral density plots of positive and negative populations based on **E12**. (D) Unmixing result of the CD24 BV510 single-stained sample using corrected spectrum calculation based on positive and negative populations with identical autofluorescence signals.

Conclusions

This application note presents a method for identifying autofluorescence in spectral flow cytometry using both fresh and stabilized human peripheral blood samples, as well as mouse spleen and lung samples. By comparing unmixing with and without the autofluorescence spectra included, we demonstrate that the impact of autofluorescence varies across sample types. Whether autofluorescence affects analysis, and to what extent, depends on its homogeneity and signal intensity. Crucially, incorporating autofluorescence spectra into unmixing improves signal resolution and analytical accuracy when autofluorescence reaches certain intensity thresholds or exhibits heterogeneity.

Overall, due to the varying autofluorescence characteristics in different samples, selecting an appropriate autofluorescence subtraction strategy is crucial for ensuring the accuracy of spectral flow cytometry unmixing results. The Agilent NovoCyte Opteon spectral flow cytometer, with its advanced capabilities and NovoExpress software, exemplifies this by treating autofluorescence as a distinct spectral feature to enable precise autofluorescence subtraction and high-resolution data acquisition.

References

1. Monici, M. Cell and tissue autofluorescence research and diagnostic applications. *Biotechnol Annu Rev*. **2005**, *11*, 227-56. DOI: 10.1016/S1387-2656(05)11007-2.
2. Ferrer-Font, L.; Small, S.J.; Lewer, B.; Pilkington, K.R.; Johnston, L.K.; Park, L.M.; Lannigan, J.; Jaimes, M.C.; Price, K.M. Panel optimization for high-dimensional immunophenotyping assay using full-spectrum flow cytometry. *Curr Protoc.* **2021**, *1*(9), e222. DOI: 10.1002/cpz1.222.
3. Mitchell, A.J.; Pradel, L.C.; Chasson, L.; Van Rooijen, N.; Grau, G.E.; Hunt, N.H.; Chimini, G. Technical advance: autofluorescence as a tool for myeloid cell analysis. *J Leukoc Biol*. **2010**, *88*(3), 597-603. DOI: 10.1189/jlb.0310184.
4. Lokwani, R.; Chaudhari, R.; Wolf, M. T.; Sadtler, K. Spectral cytometry on highly autofluorescent samples. *Nat Rev Meth Primers*. **2022**, *2*(71). DOI: 10.1038/s43586-022-00156-0.
5. Roet, J. E. G.; Mikula, A. M.; de Kok, M.; Chadick, C. H.; Garcia Vallejo, J. J.; Roest, H. P.; van der Laan, L. J. W.; de Winde, C. M.; Mebius, R. E. Unbiased method for spectral analysis of cells with great diversity of autofluorescence spectra. *Cytometry A*. **2024**, *105*(8), 595-606. DOI: 10.1002/cyto.a.24856.

Products used in this application

Agilent products

Agilent NovoCyte Opteon spectral flow cytometer

Agilent NovoExpress Software

www.agilent.com

RA260223.635

Published in the USA, March 3, 2026
5994-8794EN

Agilent
Trusted Answers